Ultra-thin Carbon Fiber Composites: Constitutive Modeling and Applications to Deployable Structures

Lectures 3-4

Sergio Pellegrino
California Institute of Technology
sergiop@caltech.edu

Outline

- Homogenization theory and elastic constitutive model for TWF
- Experimental validation
- Thermo-elastic behavior of TWF

Linear-Elastic Constitutive Model

- Kirchhoff thin plate model
- Displacement components of mid-surface: u, v, w
- Kinematic variables:

mid-plane strains

$$\varepsilon_x = \frac{\partial u}{\partial x}$$

$$\varepsilon_y = \frac{\partial v}{\partial y}$$

$$\varepsilon_{xy} = \frac{\partial u}{\partial y} + \frac{\partial v}{\partial x}$$

mid-plane curvatures

$$\kappa_x = -\frac{\partial^2 w}{\partial x^2}$$

$$\kappa_y = -\frac{\partial^2 w}{\partial y^2}$$

$$\kappa_{xy} = -2\,\frac{\partial^2 w}{\partial x \partial y}$$

Note:
We use the engineering shear strain and twice the surface twist

ABD Matrix

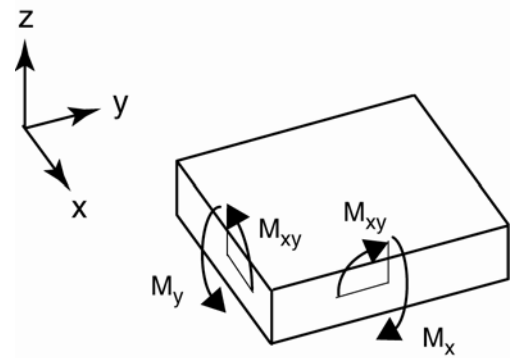

$$\begin{Bmatrix} N_x \\ N_y \\ N_{xy} \\ \hline M_x \\ M_y \\ M_{xy} \end{Bmatrix} = \left[\begin{array}{ccc|ccc} A_{11} & A_{12} & A_{16} & B_{11} & B_{12} & B_{16} \\ A_{21} & A_{22} & A_{26} & B_{21} & B_{22} & B_{26} \\ A_{61} & A_{62} & A_{66} & B_{61} & B_{62} & B_{66} \\ \hline B_{11} & B_{21} & B_{61} & D_{11} & D_{12} & D_{16} \\ B_{12} & B_{22} & B_{62} & D_{21} & D_{22} & D_{26} \\ B_{16} & B_{26} & B_{66} & D_{61} & D_{62} & D_{66} \end{array}\right] \begin{Bmatrix} \varepsilon_x \\ \varepsilon_y \\ \varepsilon_{xy} \\ \hline \kappa_x \\ \kappa_y \\ \kappa_{xy} \end{Bmatrix}$$

- A_{ij}, B_{ij}, and D_{ij} represent the in-plane (stretching and shearing), coupling, and out-of-plane (bending and twisting) stiffnesses of the plate.
- ABD matrix is symmetric and so A and D are also symmetric. However (unlike the case of a laminated plate) in general B is not symmetric.

A Simple Cartesian Unit Cell

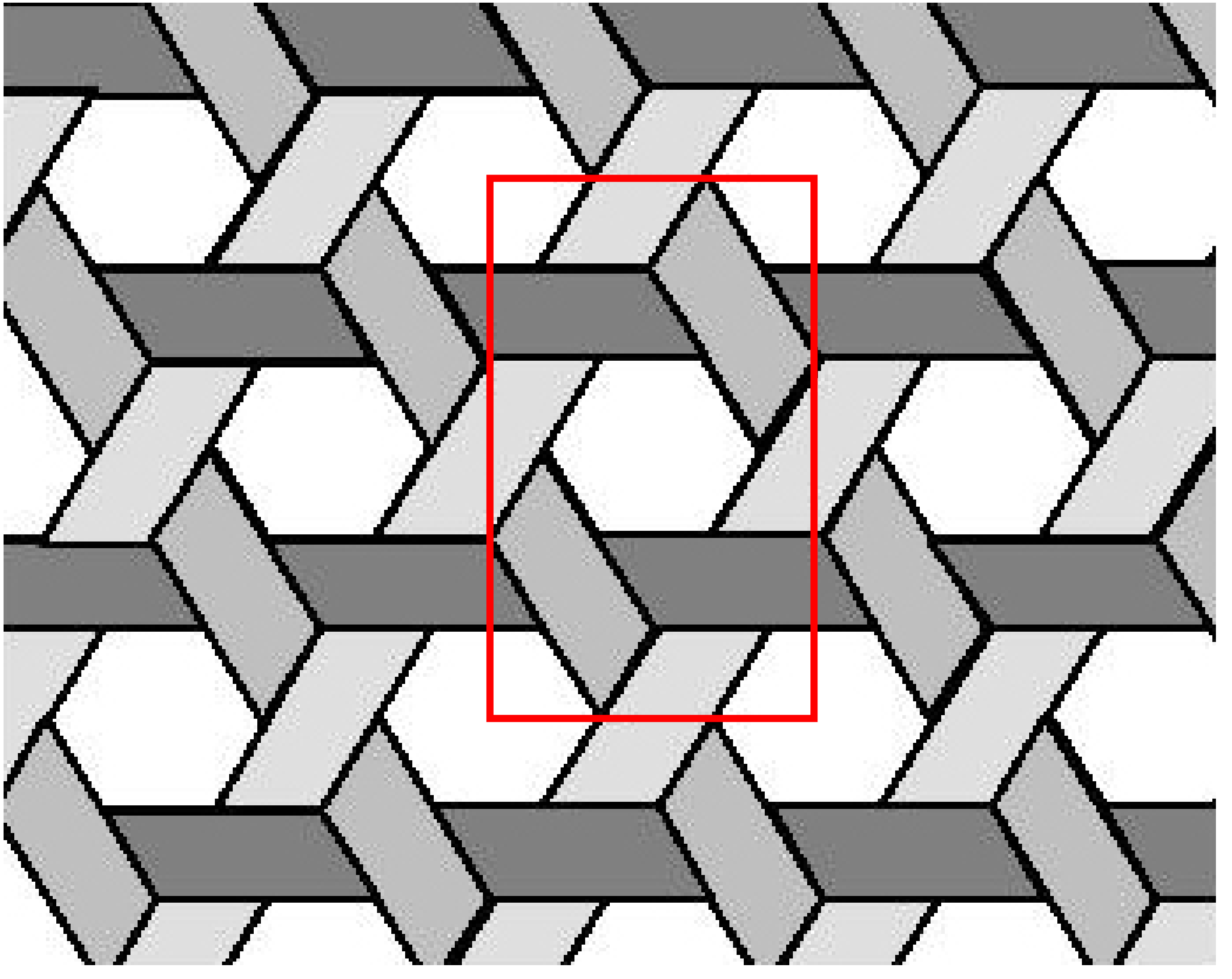

Periodic Boundary Conditions: an Engineering Approach (1)

- Expand each displacement component into a Taylor's series

$$
\begin{aligned}
u &= u_0 + \left(\frac{\partial u}{\partial x}\right)_0 x + \left(\frac{\partial u}{\partial y}\right)_0 y \\
v &= v_0 + \left(\frac{\partial v}{\partial x}\right)_0 x + \left(\frac{\partial v}{\partial y}\right)_0 y \\
w &= w_0 + \left(\frac{\partial w}{\partial x}\right)_0 x + \left(\frac{\partial w}{\partial y}\right)_0 y + \frac{1}{2}\left(\frac{\partial^2 w}{\partial x^2}\right)_0 x^2 + \left(\frac{\partial^2 w}{\partial x \partial y}\right)_0 xy + \frac{1}{2}\left(\frac{\partial^2 w}{\partial y^2}\right)_0 y^2
\end{aligned}
$$

- Then substitute the strain and curvature components

$$
\begin{aligned}
u &= u_0 + \varepsilon_x x + \frac{1}{2}\varepsilon_{xy} y \\
v &= v_0 + \frac{1}{2}\varepsilon_{xy} x + \varepsilon_y y \\
w &= -\theta_{y0} x + \theta_{x0} y - \frac{1}{2}\kappa_x x^2 - \frac{1}{2}\kappa_{xy} xy - \frac{1}{2}\kappa_y y^2
\end{aligned}
$$

Periodic Boundary Conditions: an Engineering Approach (2)

- Differentiate w to find expressions for the slopes

$$\begin{aligned}\theta_x &= \frac{\partial w}{\partial y} = \theta_{x0} - \frac{1}{2}\kappa_{xy}x - \kappa_y y \\ \theta_y &= -\frac{\partial w}{\partial x} = \theta_{y0} + \kappa_x x + \frac{1}{2}\kappa_{xy}y\end{aligned}$$

- Now consider a finite element model of our unit cell

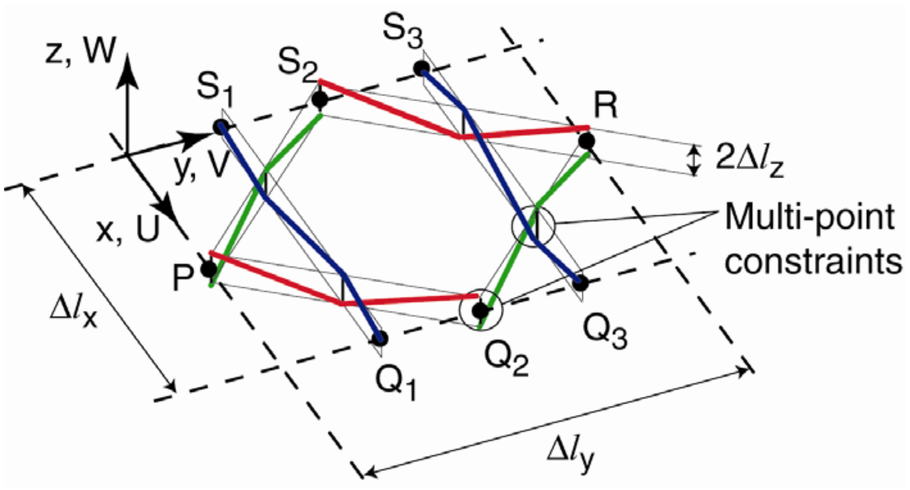

Periodic Boundary Conditions: an Engineering Approach (3)

- Consider a general pair of nodes lying on boundaries of the unit cell. The change in *in-plane displacement* between these two nodes is set equal to the deformation of two corresponding points on the homogenized plate.

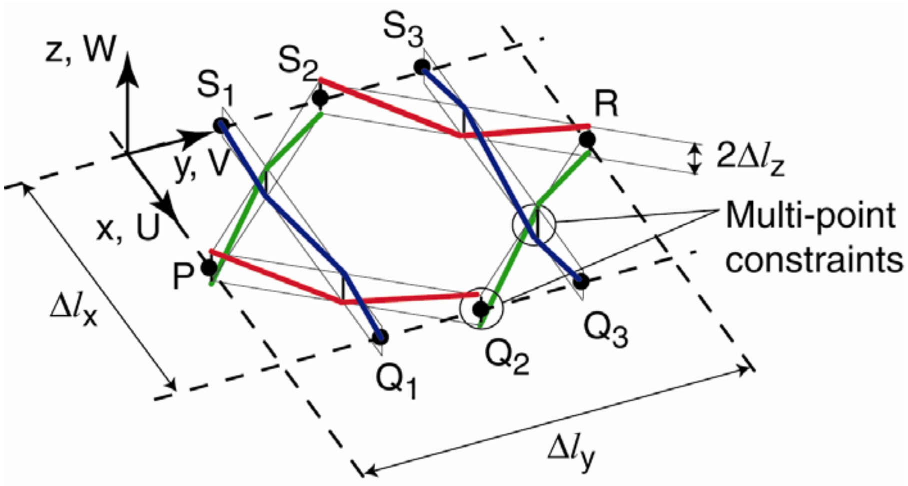

$$
\begin{aligned}
u^{Q_i} - u^{S_i} &= \varepsilon_x \Delta l_x \\
v^{Q_i} - v^{S_i} &= \frac{1}{2}\varepsilon_{xy} \Delta l_x
\end{aligned}
$$

for $i = 1, 2, 3$

$$
\begin{aligned}
u^{R} - u^{P} &= \frac{1}{2}\varepsilon_{xy} \Delta l_y \\
v^{R} - v^{P} &= \varepsilon_y \Delta l_y
\end{aligned}
$$

Periodic Boundary Conditions: an Engineering Approach (4)

- We follow the same approach for w

$$w = w_0 + \left(\frac{\partial w}{\partial x}\right)_0 x + \left(\frac{\partial w}{\partial y}\right)_0 y + \frac{1}{2}\left(\frac{\partial^2 w}{\partial x^2}\right)_0 x^2 + \left(\frac{\partial^2 w}{\partial x \partial y}\right)_0 xy + \frac{1}{2}\left(\frac{\partial^2 w}{\partial y^2}\right)_0 y^2$$

- and again substitute the strain and curvature components

$$\begin{aligned} w &= -\theta_{y0}x + \theta_{x0}y - \frac{1}{2}\kappa_x x^2 - \frac{1}{2}\kappa_{xy}xy - \frac{1}{2}\kappa_y y^2 \\ \theta_x &= \frac{\partial w}{\partial y} = \theta_{x0} - \frac{1}{2}\kappa_{xy}x - \kappa_y y \\ \theta_y &= -\frac{\partial w}{\partial x} = \theta_{y0} + \kappa_x x + \frac{1}{2}\kappa_{xy}y \end{aligned}$$

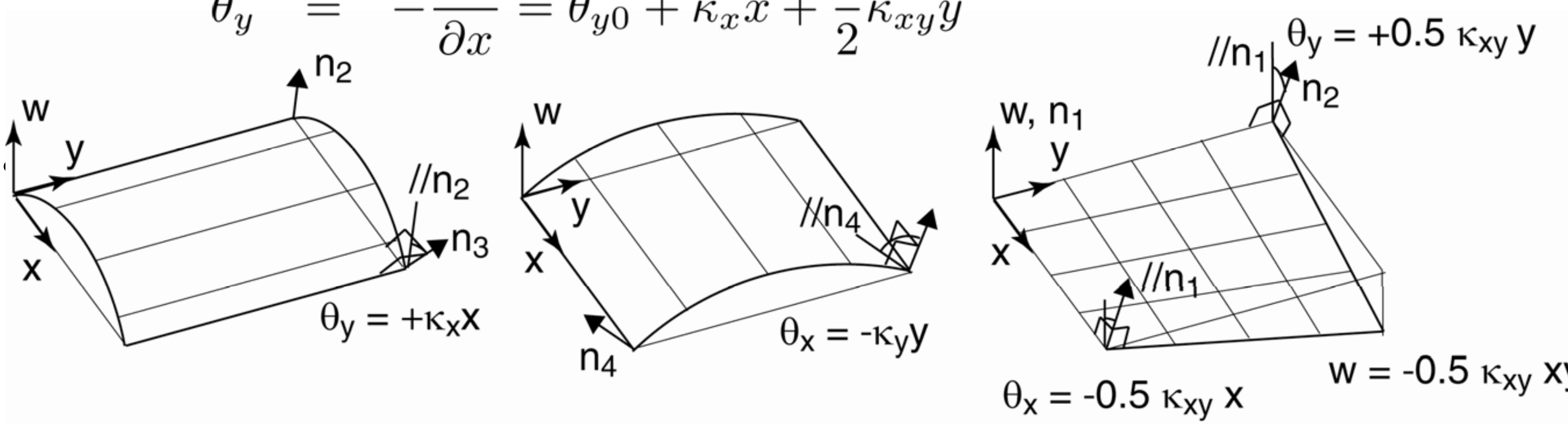

Periodic Boundary Conditions: an Engineering Approach (5)

- Substituting the coordinates of the relevant pairs of boundary nodes these compatibility equations yield

$$\begin{aligned} w^{Q_i} - w^{S_i} &= -\frac{1}{2}\kappa_{xy} y_i \Delta l_x \\ w^R - w^P &= -\frac{1}{2}\kappa_{xy}\frac{\Delta l_x}{2}\Delta l_y \end{aligned}$$

and

$$\begin{aligned} \theta_x^{Q_i} - \theta_x^{S_i} &= -\frac{1}{2}\kappa_{xy}\Delta l_x \\ \theta_y^{Q_i} - \theta_y^{S_i} &= \kappa_x \Delta l_x \\ \theta_x^R - \theta_x^P &= -\kappa_y \Delta l_y \\ \theta_y^R - \theta_y^P &= \frac{1}{2}\kappa_{xy}\Delta l_y \end{aligned}$$

- In addition, we set

$$\theta_z^R - \theta_z^P = 0 \qquad \theta_z^{Q_i} - \theta_z^{S_i} = 0$$

Unit Cell FE Model

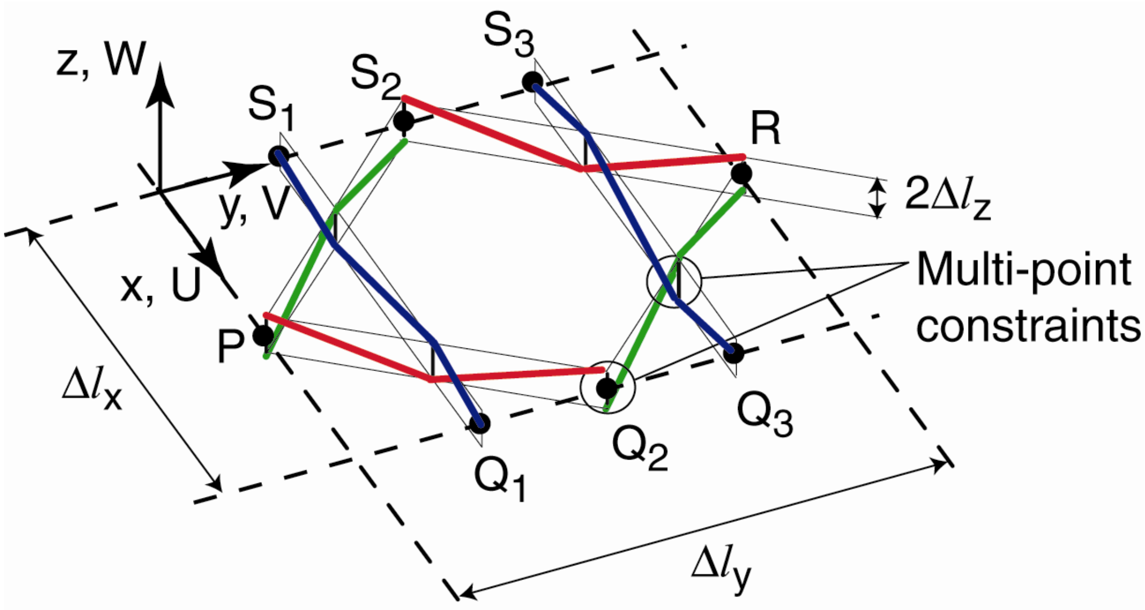

- Wavy beams with rectangular cross-section (0.803 mm x 0.078 mm)
- Rigid beam multi-point constraints (MPC)
- 8 boundary nodes on mid-plane
- Periodic boundary conditions: $\Delta u_i = \varepsilon_{ij} \Delta x_j$, $\Delta \theta_i = \kappa_{ij} \Delta x_j$

Calculation of ABD matrix

- To derive the ABD matrix six unit deformations are imposed on the unit cell, in six separate analyses.
- In each analysis a single average strain/curvature is set equal to one and all others are set equal to zero. For instance, in the first analysis, ε_x= 1 while ε_y= ε_{xy}=0 and κ_x= κ_y=κ_{xy}=0.
- Each of the six analyses provides one set of deformations, including displacement and rotation components at the 8 boundary nodes, and one set of corresponding constraint forces and moments at the same nodes.

Six Virtual Deformation Modes

$\varepsilon_{xx} = 1$

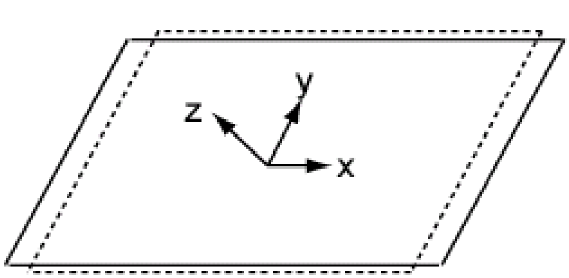

$\varepsilon_{yy} = 1$

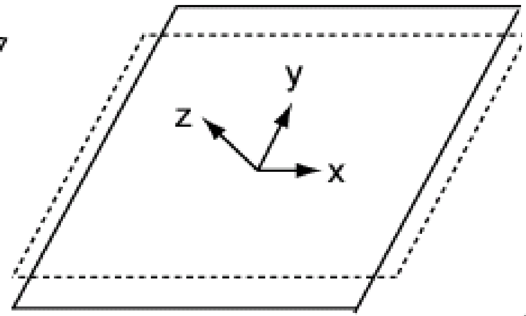

$\varepsilon_{xy} = 1$

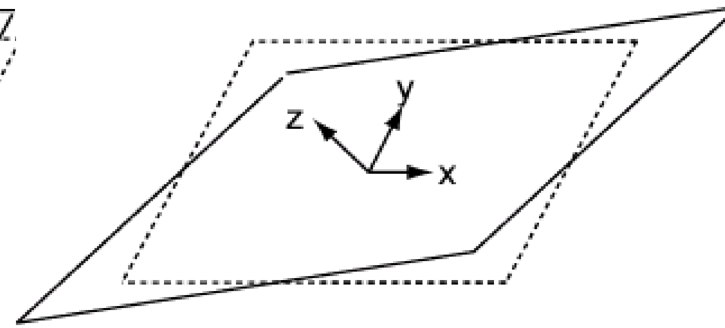

$\kappa_{xx} = 1$

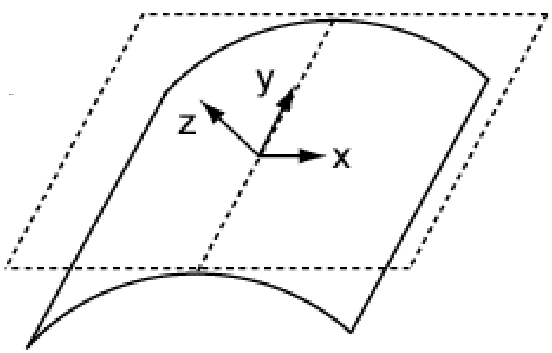

$\kappa_{yy} = 1$

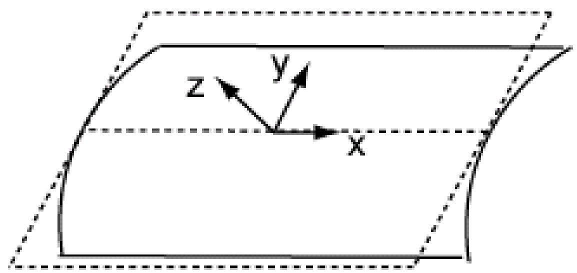

$\kappa_{xy} = 1$

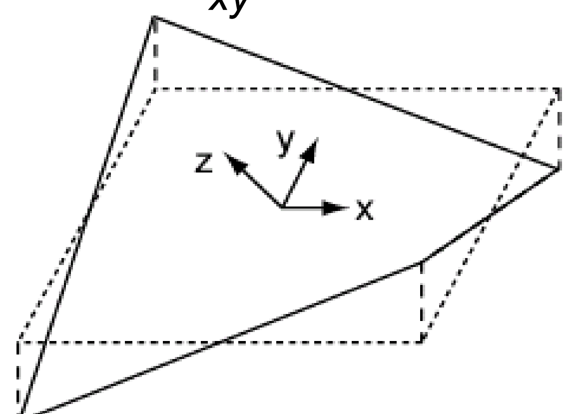

Virtual work computation of ABD matrix

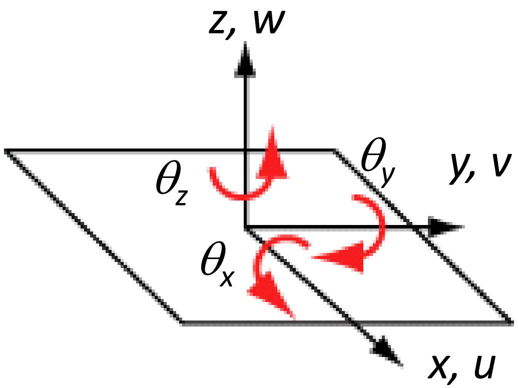

- Entry [1,1] of ABD matrix, A_{11}

$$N_{xx}\varepsilon_{xx}\Delta l_x \Delta l_y = \sum_{b.n.} (F_x u + F_y v + F_z w + M_x\theta_x + M_y\theta_y + M_z\theta_z)$$

- since ε_{xx} = 1,

$$A_{11} = \frac{\sum_{b.n.} (F_x u + F_y v + F_z w + M_x\theta_x + M_y\theta_y + M_z\theta_z)}{\Delta l_x \Delta l_y}$$

Results of 6 FE Analyses (A, B, C,…)

Boundary node displ. & rotns

$$U = \begin{bmatrix} u_{PA} & u_{PB} & u_{PC} & u_{PD} & u_{PE} & u_{PF} \\ v_{PA} & v_{PB} & v_{PC} & v_{PD} & v_{PE} & v_{PF} \\ w_{PA} & w_{PB} & w_{PC} & w_{PD} & w_{PE} & w_{PF} \\ \theta_{PxA} & \theta_{PxB} & \theta_{PxC} & \theta_{PxD} & \theta_{PxE} & \theta_{PxF} \\ \theta_{PyA} & \theta_{PyB} & \theta_{PyC} & \theta_{PyD} & \theta_{PyE} & \theta_{PyF} \\ \theta_{PzA} & \theta_{PzB} & \theta_{PzC} & \theta_{PzD} & \theta_{PzE} & \theta_{PzF} \\ u_{Q_1A} & u_{Q_1B} & u_{Q_1C} & u_{Q_1D} & u_{Q_1E} & u_{Q_1F} \\ \dots & \dots & \dots & \dots & \dots & \dots \\ \theta_{S_3zA} & \theta_{S_3zB} & \theta_{S_3zC} & \theta_{S_3zD} & \theta_{S_3zE} & \theta_{S_3zF} \end{bmatrix}$$

Boundary node force & couples

$$F = \begin{bmatrix} F_{PxA} & F_{PxB} & F_{PxC} & F_{PxD} & F_{PxE} & F_{PxF} \\ F_{PyA} & F_{PyB} & F_{PyC} & F_{PyD} & F_{PyE} & F_{PyF} \\ F_{PzA} & F_{PzB} & F_{PzC} & F_{PzD} & F_{PzE} & F_{PzF} \\ C_{PxA} & C_{PxB} & C_{PxC} & C_{PxD} & C_{PxE} & C_{PxF} \\ C_{PyA} & C_{PyB} & C_{PyC} & C_{PyD} & C_{PyE} & C_{PyF} \\ C_{PzA} & C_{PzB} & C_{PzC} & C_{PzD} & C_{PzE} & C_{PzF} \\ F_{Q_1xA} & F_{Q_1xB} & F_{Q_1xC} & F_{Q_1xD} & F_{Q_1xE} & F_{Q_1xF} \\ \dots & \dots & \dots & \dots & \dots & \dots \\ C_{S_3zA} & C_{S_3zB} & C_{S_3zC} & C_{S_3zD} & C_{S_3zE} & C_{S_3zF} \end{bmatrix}$$

And the final outcome is…

- General expression: $ABD = \frac{U^T F}{\Delta l_x \cdot \Delta l_y}$
- And for TWF this gives:

$$\begin{Bmatrix} N_x \\ N_y \\ N_{xy} \\ \hline M_x \\ M_y \\ M_{xy} \end{Bmatrix} = \left[\begin{array}{ccc|ccc} 3312 & 1991 & 0 & 0.00 & 0.00 & -0.62 \\ 1991 & 3312 & 0 & 0.00 & 0.00 & 0.62 \\ 0 & 0 & 660 & 0.62 & -0.62 & 0.00 \\ \hline 0.00 & 0.00 & 0.62 & 2.11 & 0.59 & 0.00 \\ 0.00 & 0.00 & -0.62 & 0.59 & 2.11 & 0.00 \\ -0.62 & 0.62 & 0.00 & 0.00 & 0.00 & 0.76 \end{array}\right] \begin{Bmatrix} \varepsilon_x \\ \varepsilon_y \\ \varepsilon_{xy} \\ \hline \kappa_x \\ \kappa_y \\ \kappa_{xy} \end{Bmatrix}$$

where the units are N and mm

Symmetry Properties

$$\left\{\begin{array}{c} N_x \\ N_y \\ N_{xy} \\ \hline M_x \\ M_y \\ M_{xy} \end{array}\right\} = \left[\begin{array}{ccc|ccc} 3312 & 1991 & 0 & 0.00 & 0.00 & -0.62 \\ 1991 & 3312 & 0 & 0.00 & 0.00 & 0.62 \\ 0 & 0 & 660 & 0.62 & -0.62 & 0.00 \\ \hline 0.00 & 0.00 & 0.62 & 2.11 & 0.59 & 0.00 \\ 0.00 & 0.00 & -0.62 & 0.59 & 2.11 & 0.00 \\ -0.62 & 0.62 & 0.00 & 0.00 & 0.00 & 0.76 \end{array}\right] \left\{\begin{array}{c} \varepsilon_x \\ \varepsilon_y \\ \varepsilon_{xy} \\ \hline \kappa_x \\ \kappa_y \\ \kappa_{xy} \end{array}\right\}$$

Quasi-isotropic conditions

$$A_{11} = A_{22}, \quad A_{66} = (A_{11} - A_{12})/2$$

$$D_{11} = D_{22}, \quad D_{66} = (D_{11} - D_{12})/2$$

Inverse of ABD Matrix

$$\left\{\begin{array}{c}\varepsilon_x\\ \varepsilon_y\\ \varepsilon_{xy}\\ \hline \kappa_x\\ \kappa_y\\ \kappa_{xy}\end{array}\right\} = 10^6 \times \left[\begin{array}{ccc|ccc} 473 & -284 & 0 & 0 & 0 & 614\\ -284 & 473 & 0 & 0 & 0 & -614\\ 0 & 0 & 1515 & -614 & 614 & 0\\ \hline 0 & 0 & -614 & 514086 & -143070 & 0\\ 0 & 0 & 614 & -143070 & 514086 & 0\\ 614 & -614 & 0 & 0 & 0 & 1314268\end{array}\right]\left\{\begin{array}{c}N_x\\ N_y\\ N_{xy}\\ \hline M_x\\ M_y\\ M_{xy}\end{array}\right\}$$

Experimental Validation of Constitutive Model

Size Effects

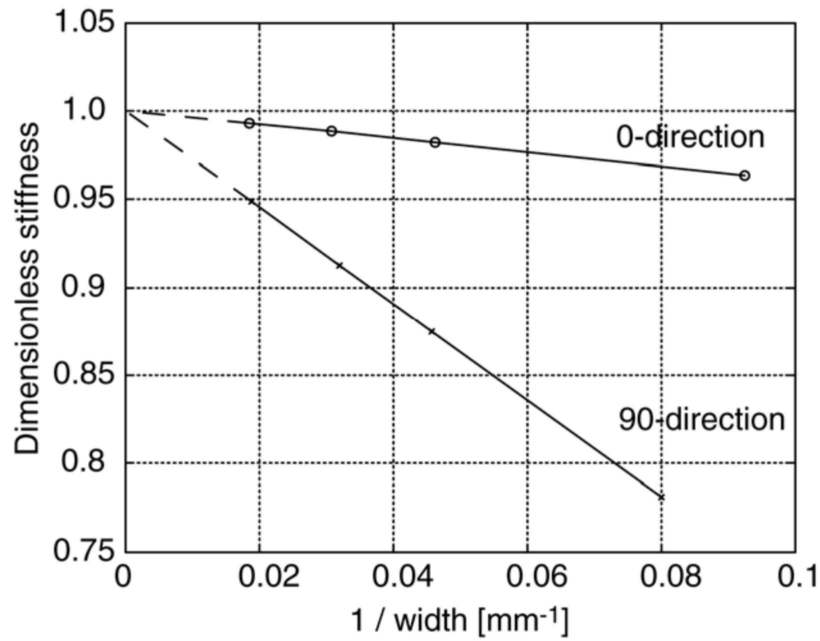

- Less sensitive in 0-direction, hence we test 0-direction specimens to obtain "material" characterization
- Edge effects in actual structures will need additional characterization

Tension Test - I

- Square test area
- Additional TWF layers act as reinforcement near tabs
- Loading rate: 1 mm/min
- Measure displacement of retro-reflective strips with laser extensometers

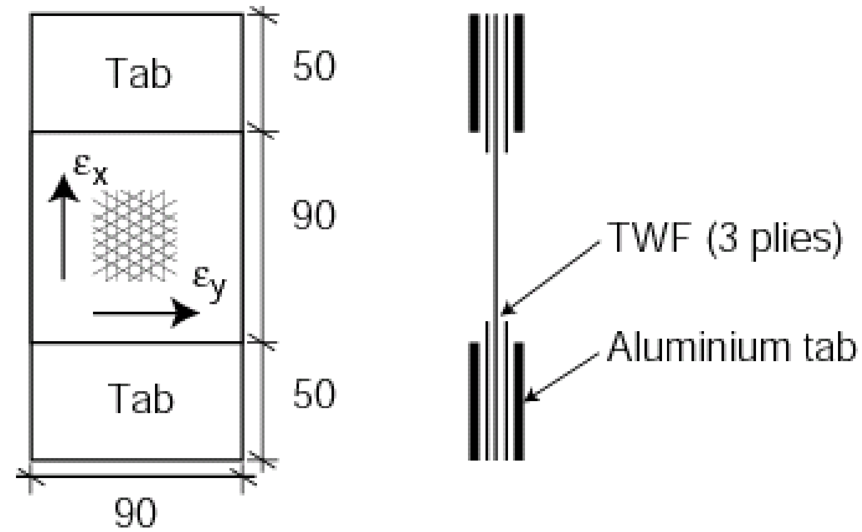

Front view *Side view*

Dimensions in mm

Tension Test - II

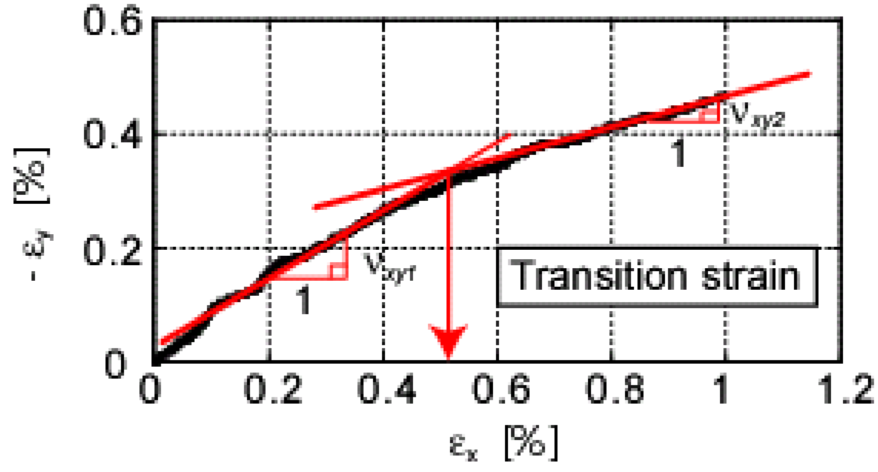

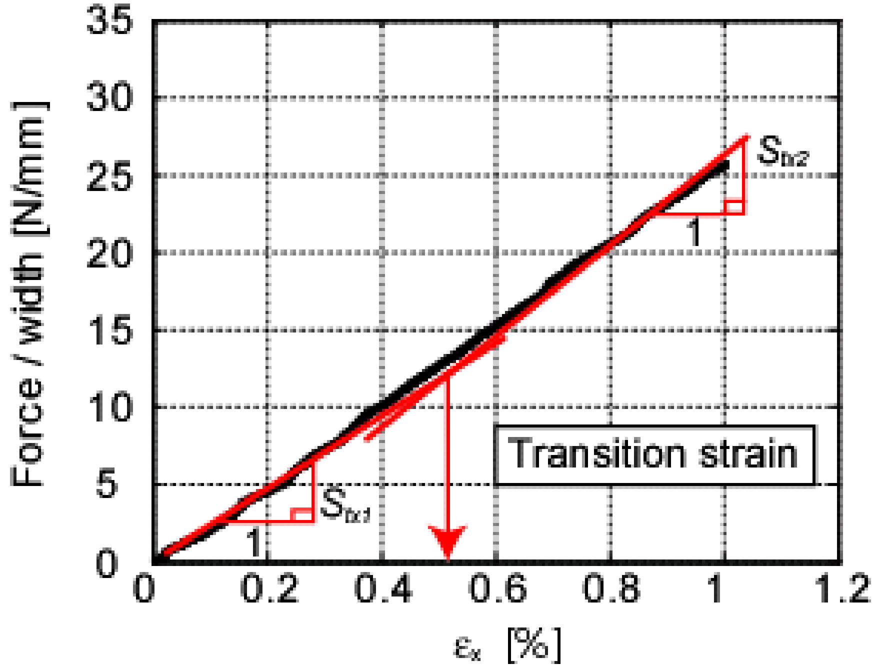

Compression Test

- Failure should be by fibre microbuckling
- Sandwich of 40 mm x 55 mm TWF and PVC foam core
- Loading rate: 1 mm/min
- Contraction along *x*-axis measured by laser extensometer

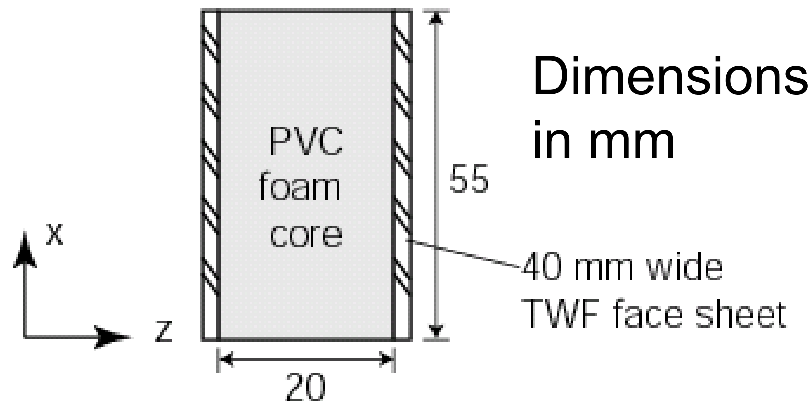

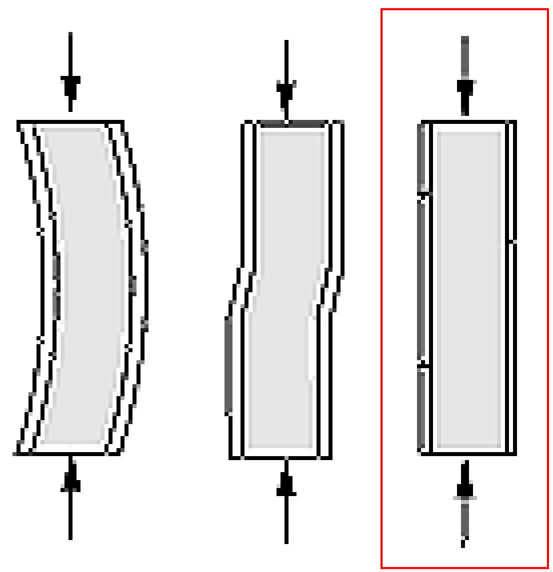

a b c d

Compression Force/Width vs Longitudinal Strain

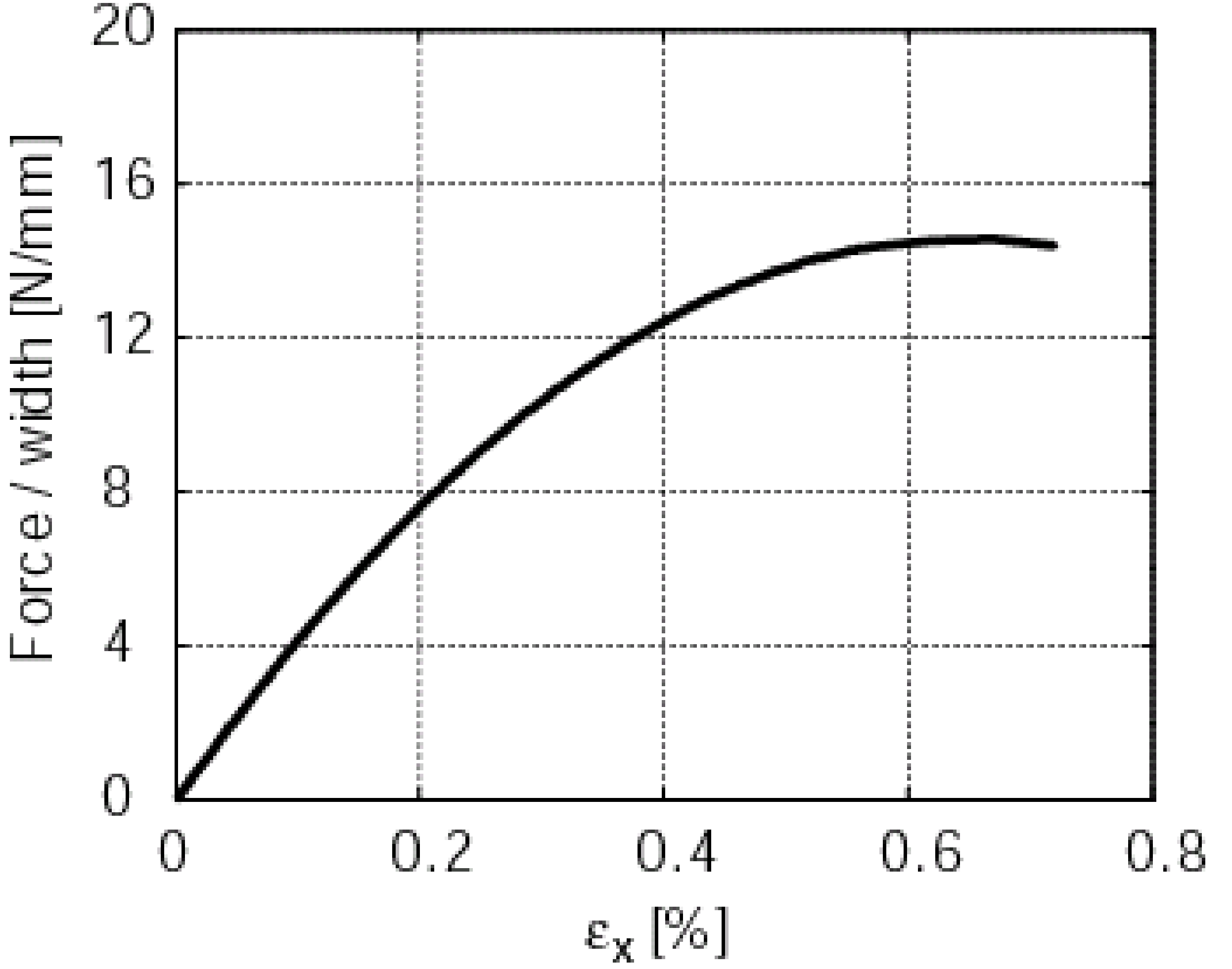

In-plane Shear Test

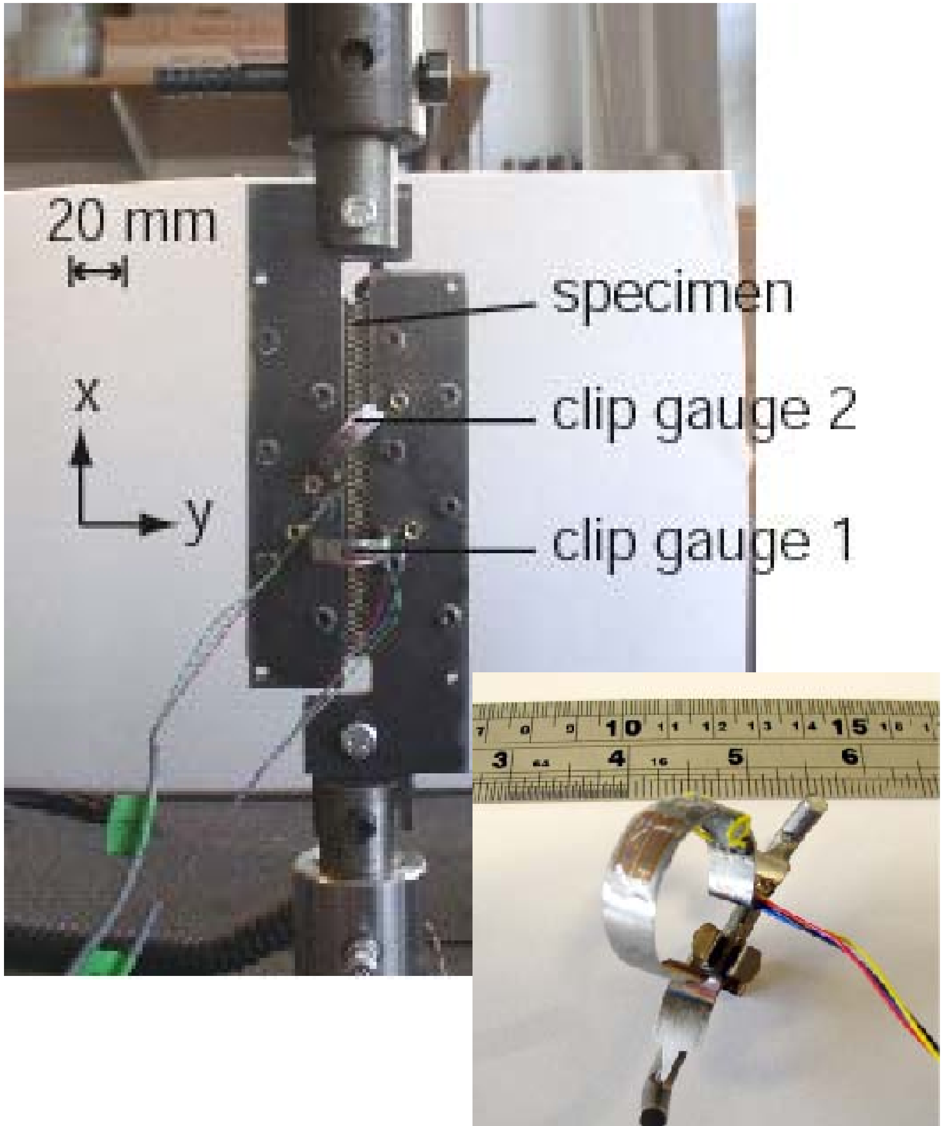

- Modified 2-rail shear rig
- 130 mm long sandwich specimen (PVC foam core)
- Loading rate: 0.5 mm/min
- Strains at 0º and 45º measured by clip gauges

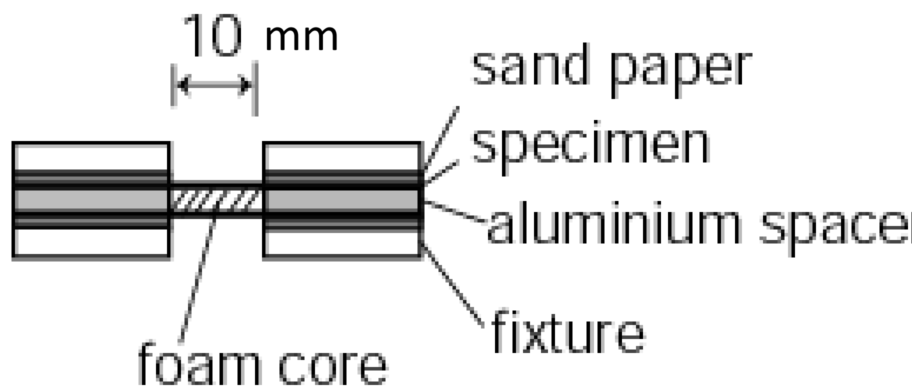

Shear Force / Length vs Shear Strain

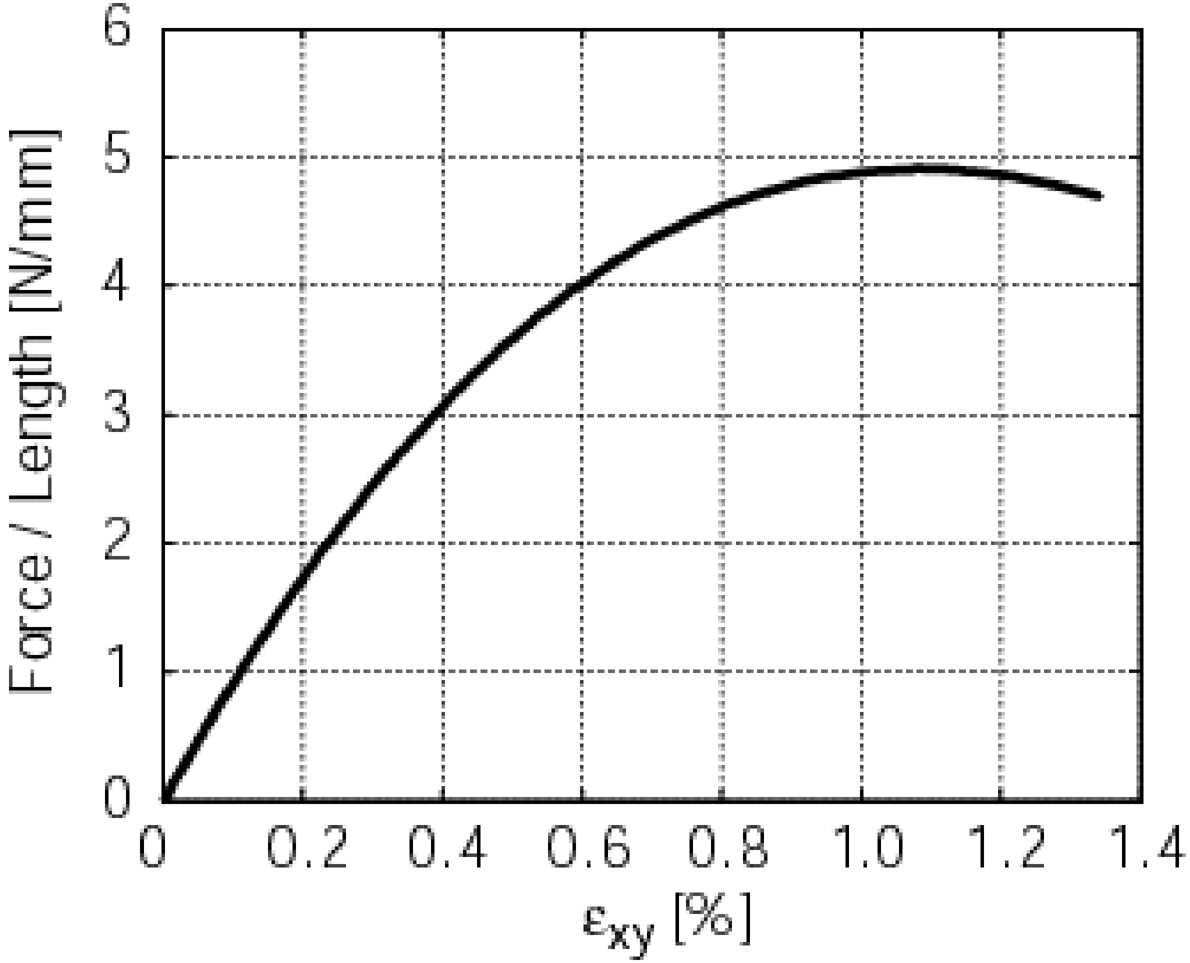

Bending Test

- 4-point bending to achieve uniform curvature
- 100 mm x 40 mm specimen
- Loading rate: 1 mm/min
- Mid-span deflection measured with laser extensometer

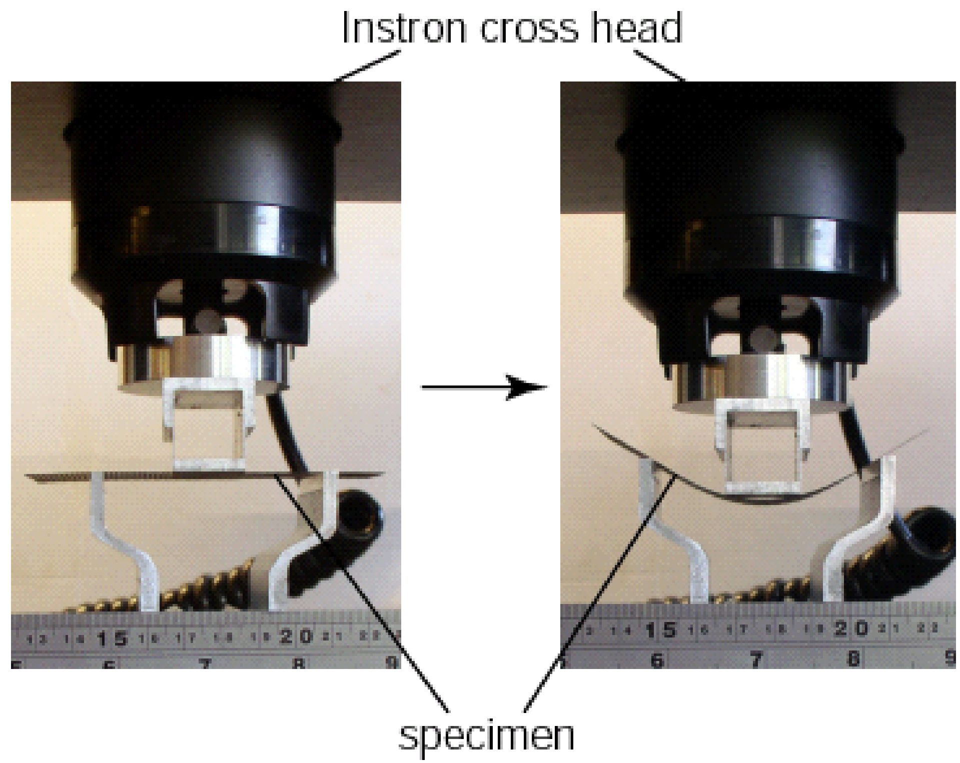

Moment / Width vs Curvature

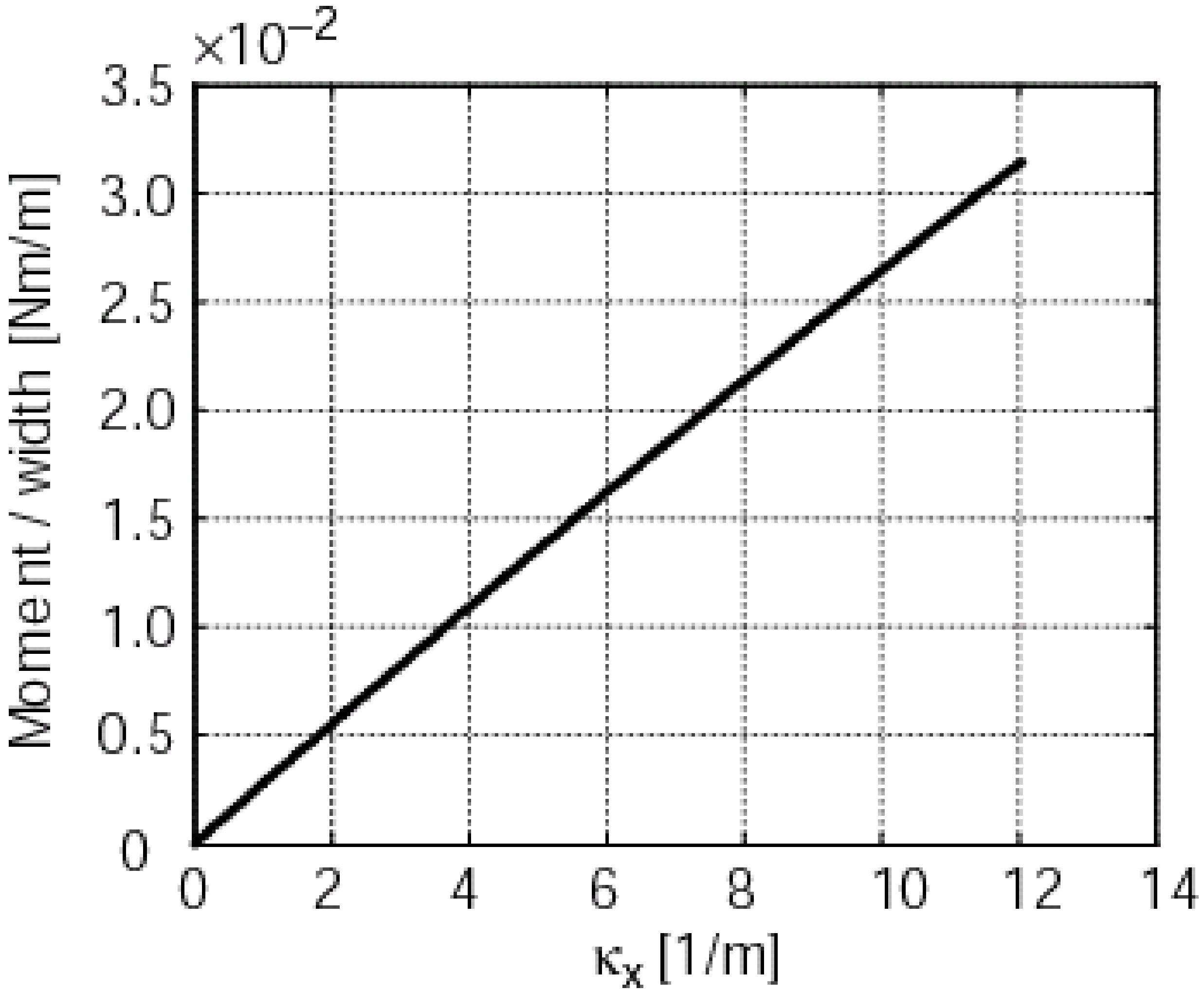

Failure Curvature

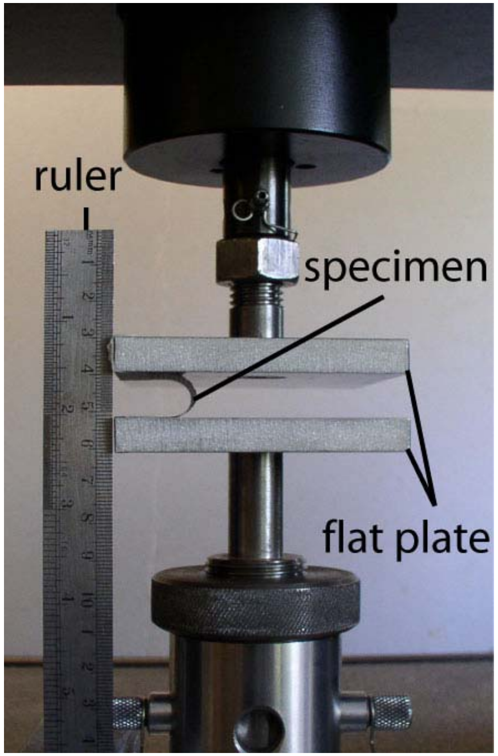

- Tests on 40 mm wide by 50 mm long specimens
- Recorded with a video camera

	Minimum radius, [mm]
Average	2.636
Std. dev.	0.076

ABD Matrix Comparison

Property	Prediction	Measurement (average)	Deviation [%]
Extensional stiffness, S_x [N/mm]	2114	2178	1
Poisson's ratio, ν_{xy}	0.601	0.6	3
Shear stiffness, S_{xy} [N/mm]	660	777	14
Bending stiffness, D_x [Nmm]	1.945	2.077	4

Thermo-Mechanical Behavior

Background

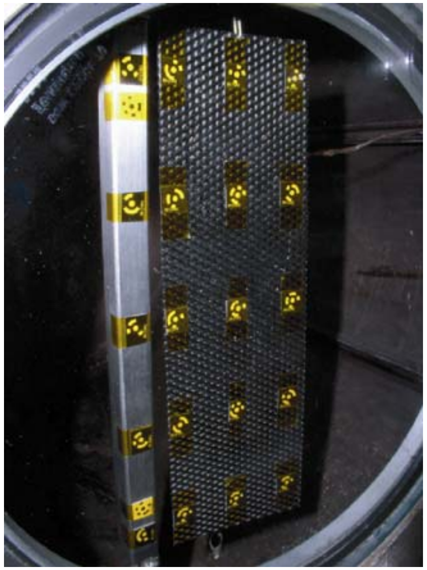

- x axis is vertical, y axis is horizontal
- Thermal deformation tests on 200 mm x 90 mm specimens showed evidence of ***thermal buckling***

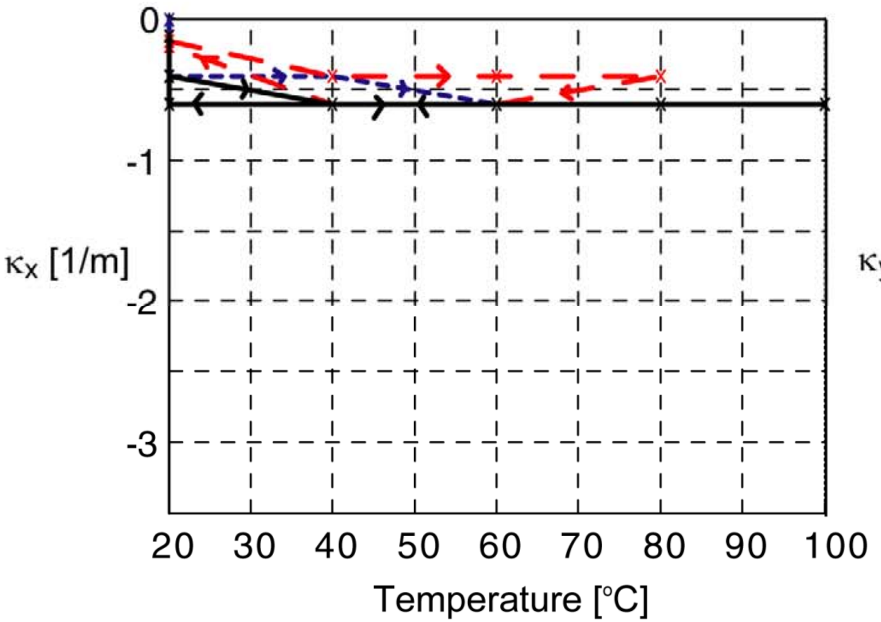

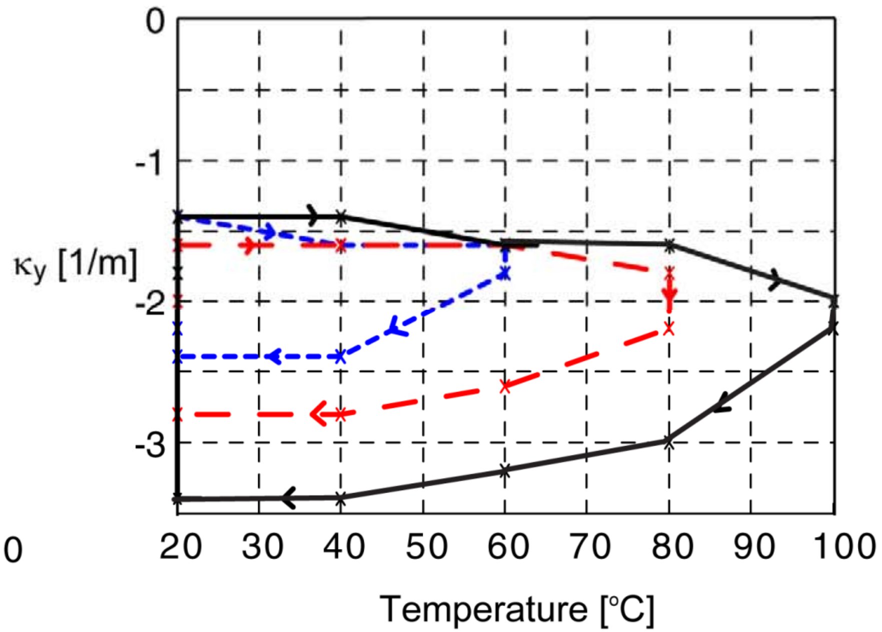

CTE Tests

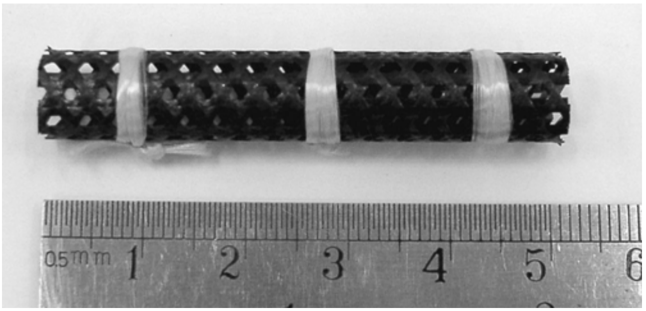

- 50 mm long cylindrical specimens wrapped with Kevlar cord
- WSK TMA 500 dilatometer
- Tests carried out by Dr Leri Datashvili at TU Munich

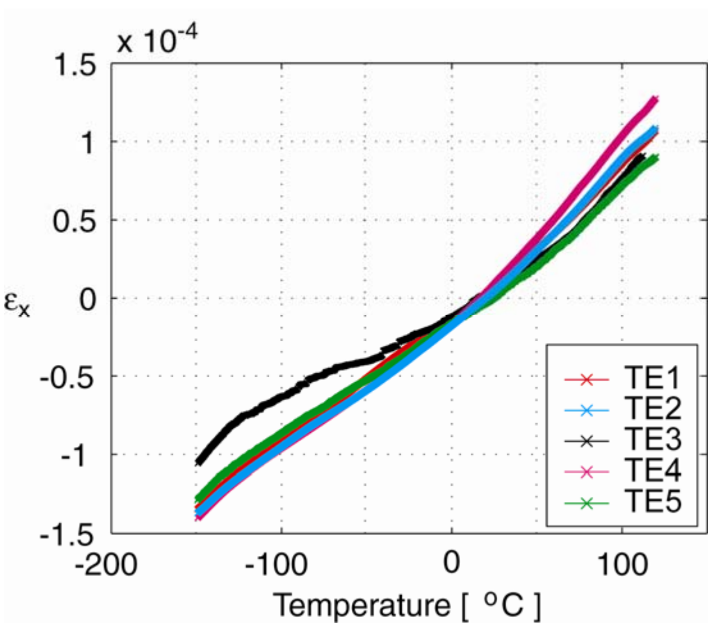

Specimen	CTE $\times 10^{-6}$ [/°C]
TE1	1.067
TE2	0.664
TE3	0.969
TE4	0.969
TE5	1.117
Average	0.957
Std. dev.	0.176
Variation [%]	18.38

Thermal Twist Tests

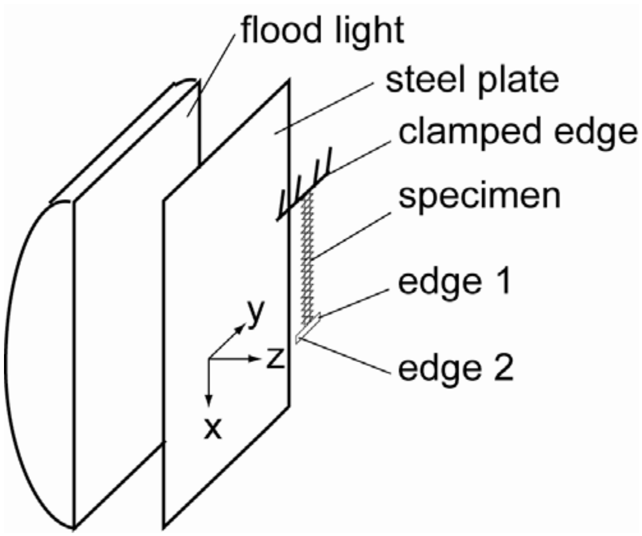

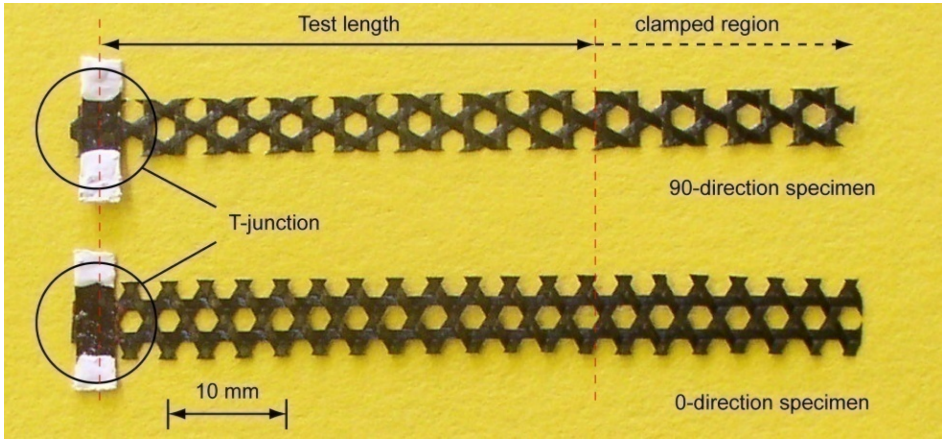

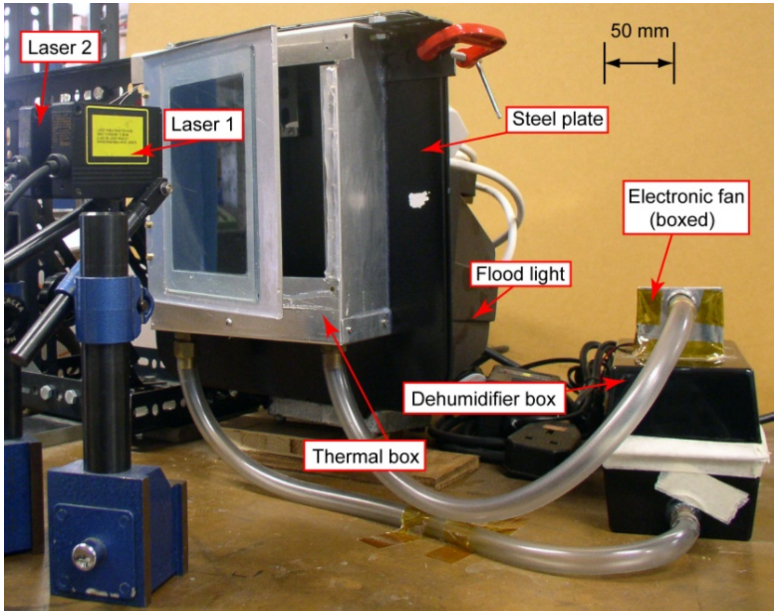

- Specimens held in vacuum for 24 hours
- Radiant heating
- Dry chamber

Tip Deflections

0-direction specimen

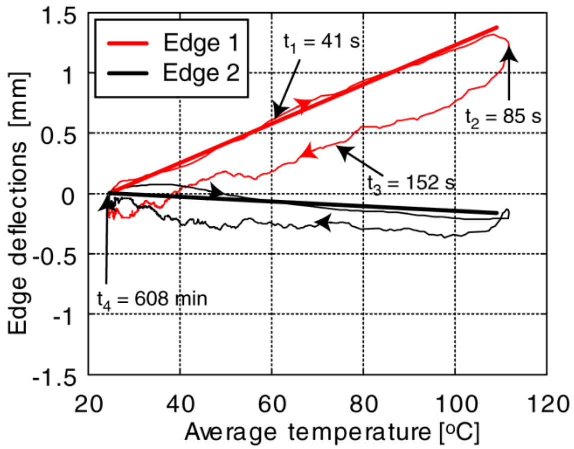

(a)

90-direction specimen

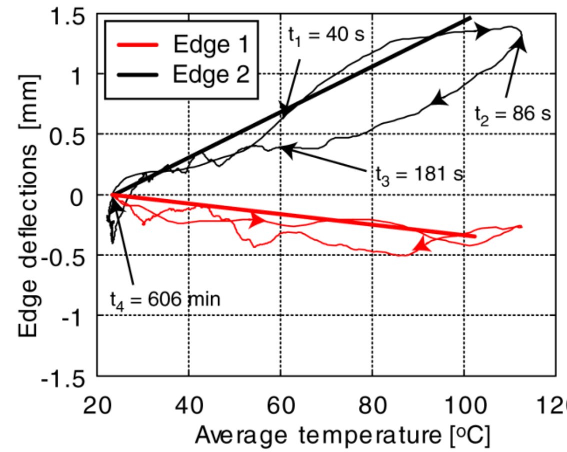

(a)

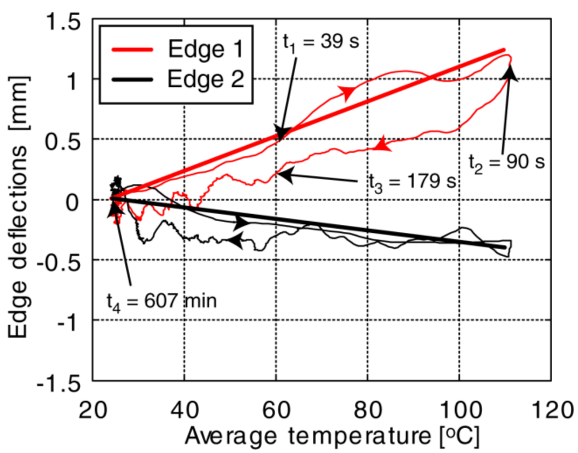

(b)

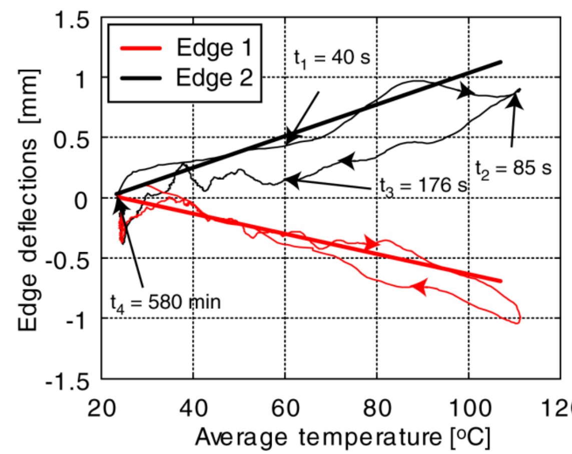

(b)

Two sets of specimens tested

Tip Deflections due to Positive Twisting Curvature

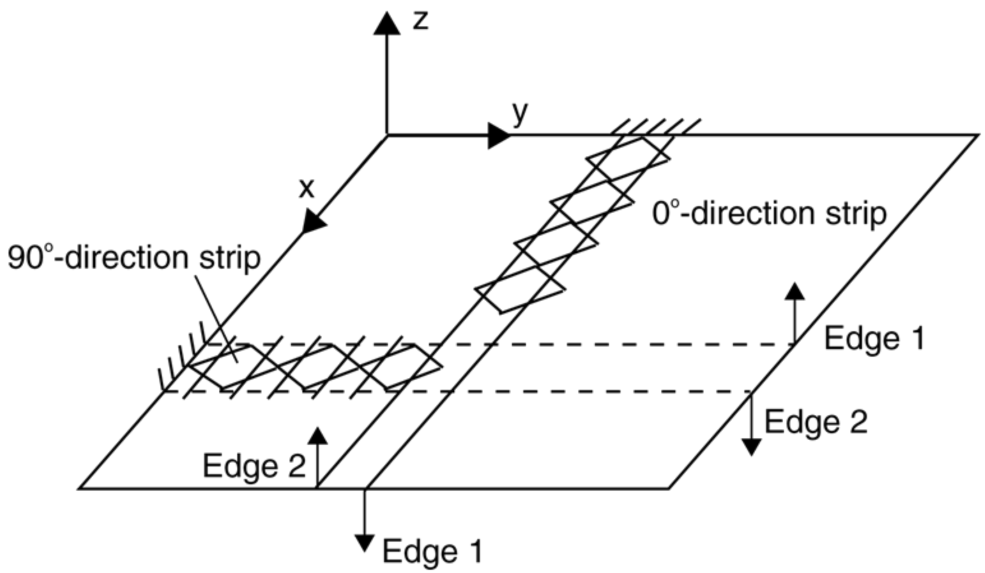

Coefficient of Thermal Twist

- The corresponding twist per unit length of each strip, or Coefficient of Thermal Twist, β, can be determined by dividing the twisting curvature

$$\kappa_{xy} = -2\,\frac{\partial^2 w}{\partial x \partial y}$$

- by the total temperature change, hence

$$\beta = -2\frac{\Delta w}{dL\Delta T}$$

Δw	=	difference in out-of-plane deflection between two tip edges
d	=	distance between edge points measured by two lasers (9.1 mm in both strips)
L	=	strip length
ΔT	=	change of temperature

Values of β

Specimen	β_0	β_{90}
TT1	-6.910E-05	-8.809E-05
TT2	-7.254E-05	-9.211E-05
TT3	-7.491E-05	-9.111E-05
Average	-7.218E-05	-9.044E-05
Std. dev.	2.921E-06	2.093E-06
Variation [%]	4.05	2.31

(units mm^{-1} $^{o}C^{-1}$)

CTE of a Single Tow

- The longitudinal thermal expansion coefficient is derived from

$$\alpha_1 = \frac{E_{1f}\alpha_{1f}V_f + E_m\alpha_m V_m}{E_{1f}V_f + E_m V_m}$$

and the transverse thermal expansion coefficient from

$$\alpha_2 = \alpha_3 = V_f\alpha_{2f}\left(1 + \nu_{12f}\frac{\alpha_{1f}}{\alpha_{2f}}\right) + V_m\alpha_m(1 + \nu_m) - (\nu_{12f}V_f + \nu_m V_m)\alpha_1$$

- Substituting our tow properties we obtain

Longitudinal CTE, α_1 [/^{o}C]	**0.16×10^{-6}**
Transverse CTE, α_2 [/^{o}C]	37.61×10^{-6}

- The longitudinal CTE we measured is 1×10^{-6}. Out by a factor of 6.

Analytical Prediction of CTE of Woven Tow

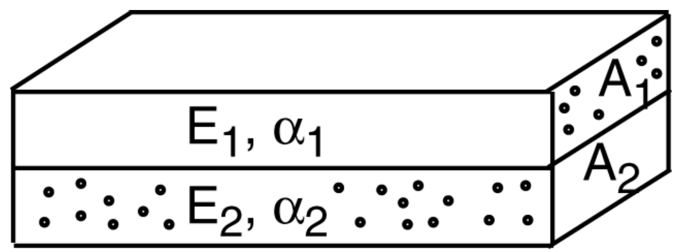

- Consider a straight tow with longitudinal CTE α_1 and modulus E_1, perfectly bonded to a series of perpendicular tows. Their CTE in the direction of the first tow is α_2 and the modulus E_2.
- The CTE of this composite is

$$\alpha_c = \left[\alpha_1 + \frac{(EA)_2(\alpha_2 - \alpha_1)}{(EA)_1 + (EA)_2} \right]$$

- Assuming 2/3 coverage of each tow by a *perpendicular* tow, we predict α=2.2 x 10^{-6} /^{o}C

Analytical prediction of CTT

- The first attempt used the wavy beam model of a 0-direction specimen to predict the thermal twist

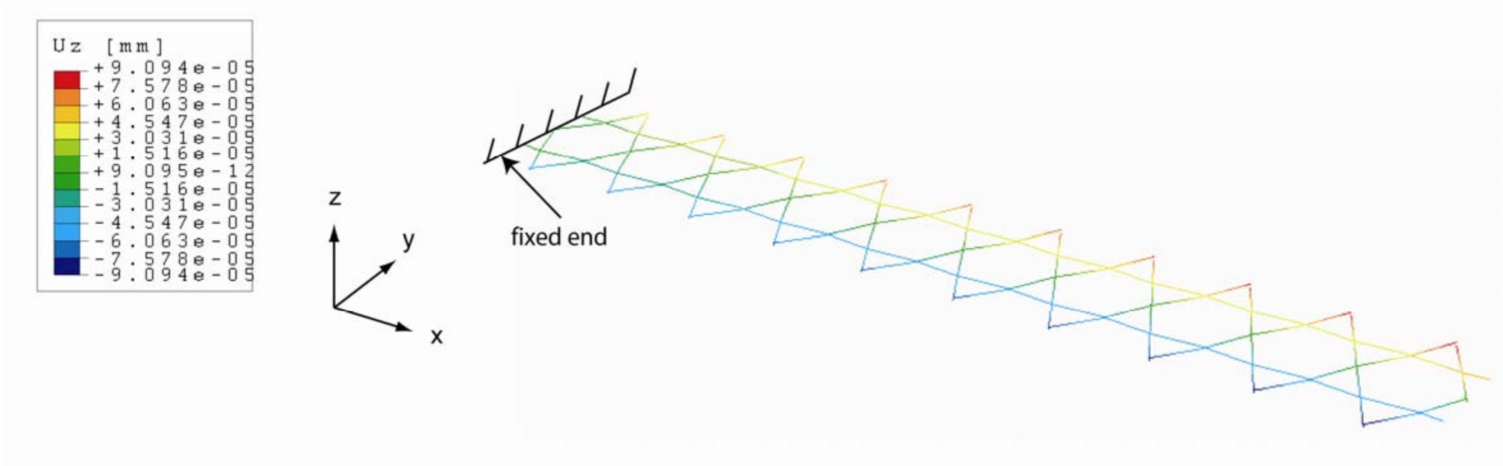

- This gave -1.136 x 10^{-8} /mm ^{o}C which is much smaller than the measured value.

Actual Deformation is 3D!

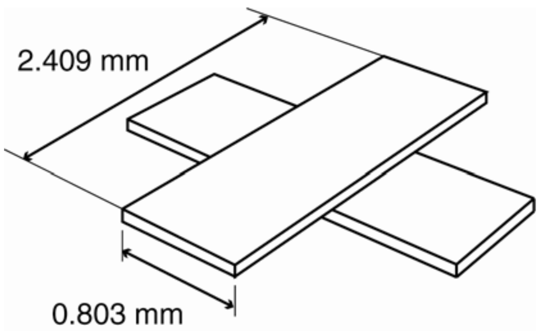

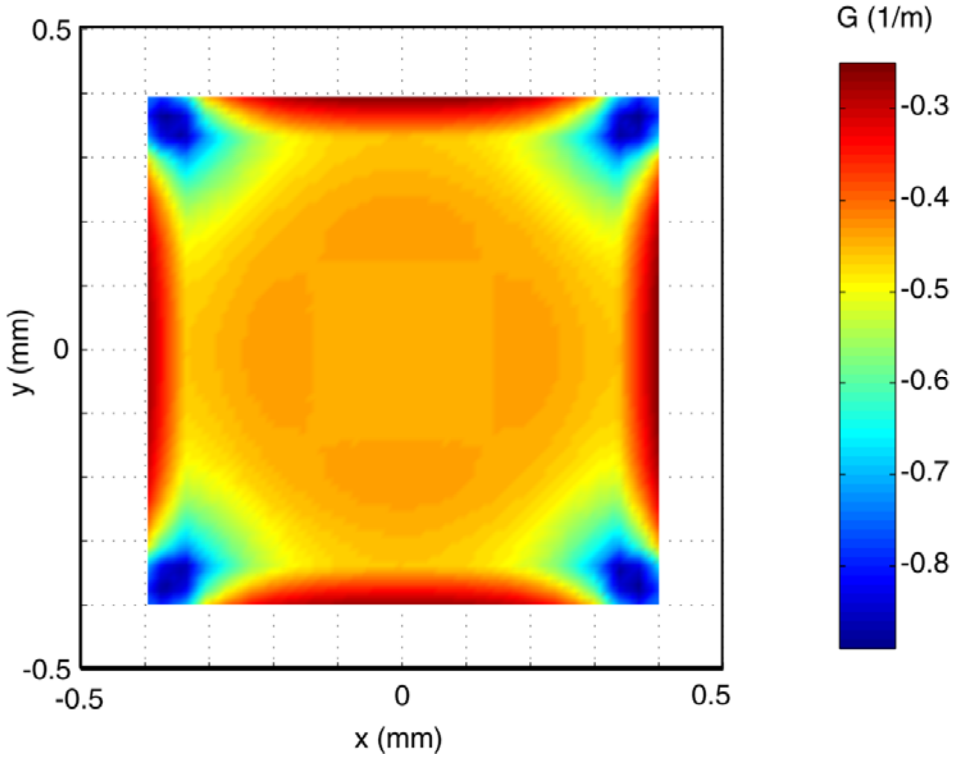

- Gaussian curvature of tow interface due to $\Delta T = 100\ ^oC$
- Analysis of two straight tows at 90 degrees shows
  - contact region deforms into a saddle
  - tows become transversally curved

Some More Realistic Geometries

Node	Type of constraint
A	Uz = 0
B	Uy, Uz = 0
C	Ux, Uy, Uz = 0

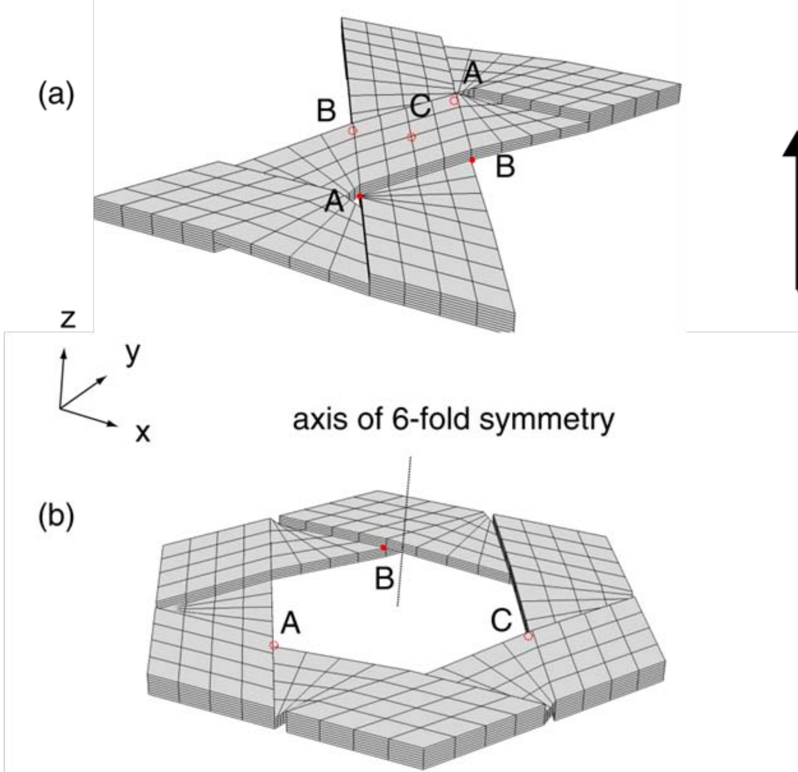

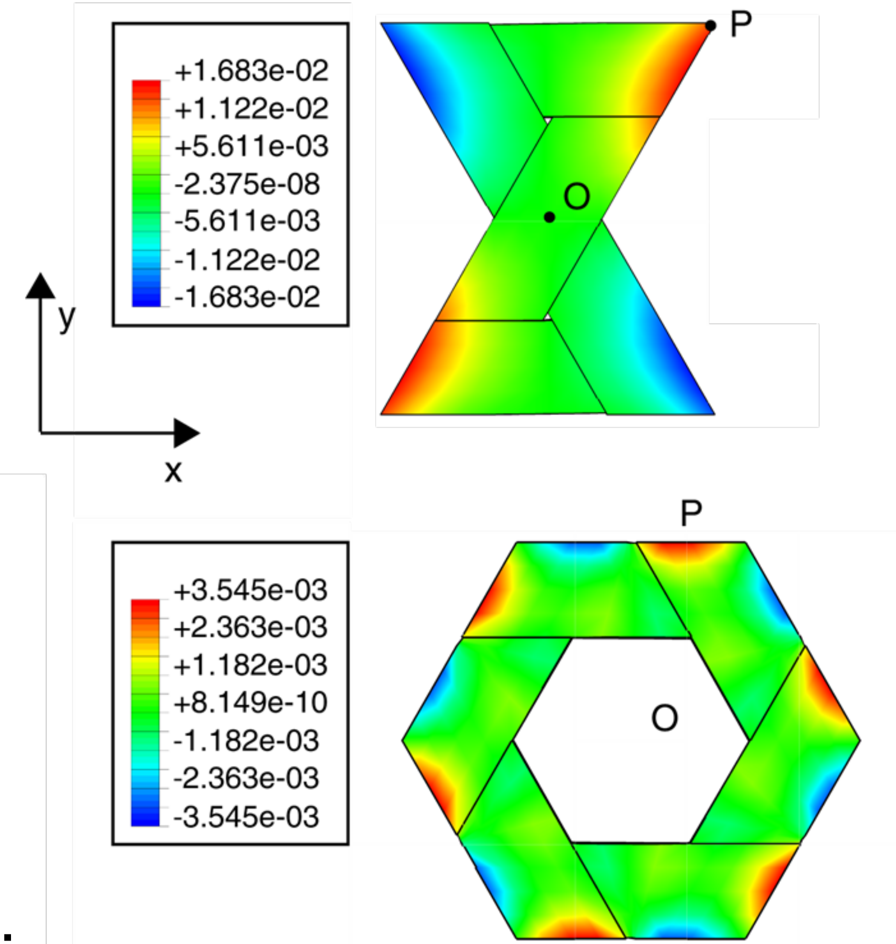

Twisting curvature of hexagonal cell:

$$\frac{\kappa_{xy}}{\Delta T} \approx -2\frac{\Delta w}{\Delta x \Delta y}\ \frac{1}{\Delta T} = -2\frac{3.545\times 10^{-3}}{0.58\times 2.7}\ \frac{1}{100} = -4.53\times 10^{-5}\ \mathrm{mm}^{-1}\ {}^\circ\mathrm{C}^{-1}$$

Two kinds of strips

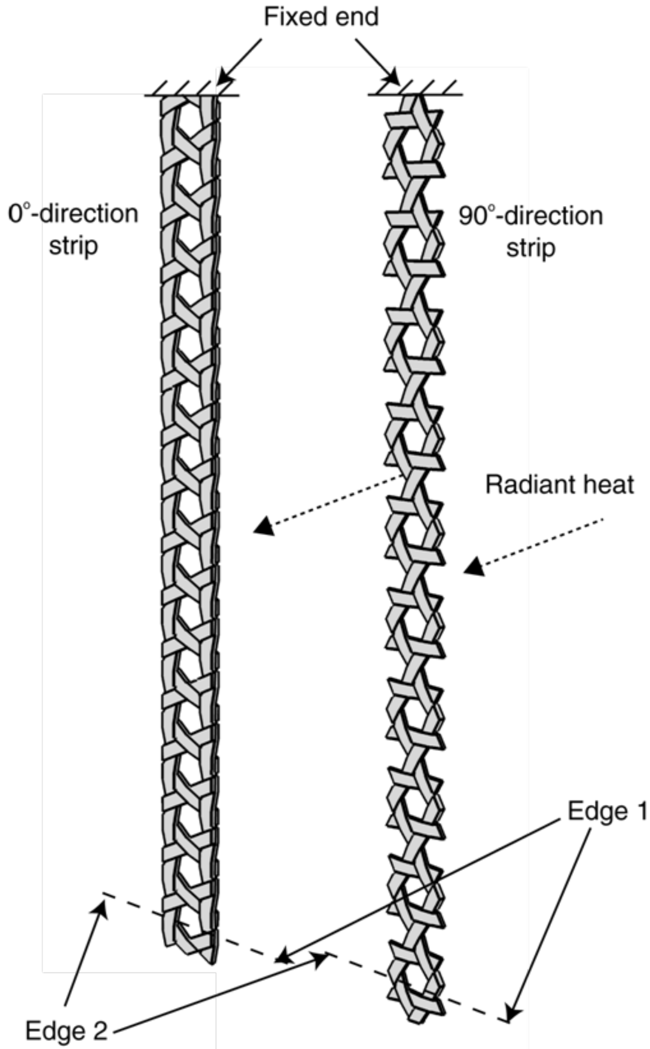

- Two load cases:
  - uniform temperature distribution or linearly varying through thickness
- First cell “clamped”
- Results insensitive to details of boundary conditions

Edge Deflections (0-direction)

Uniform ΔT of 100°C

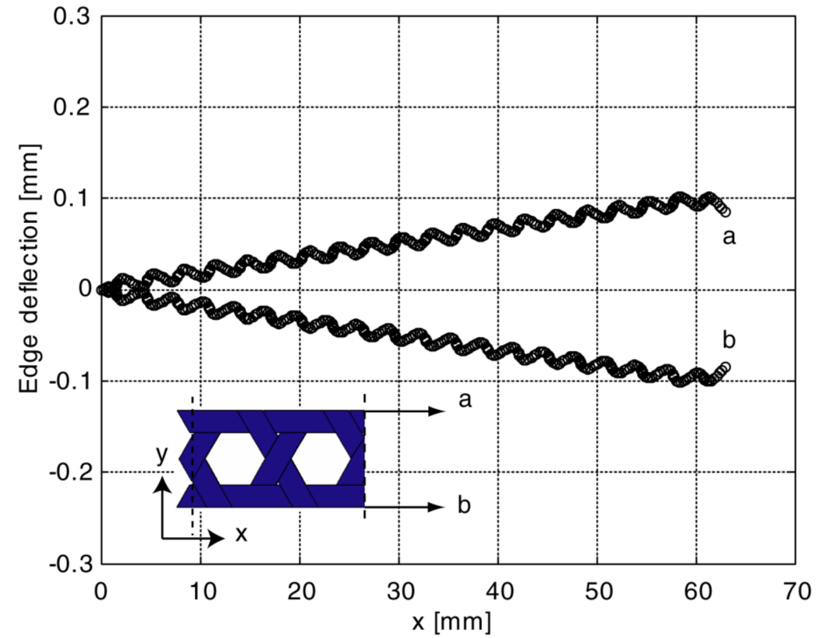

(a)

Gradient of +/- 2°C

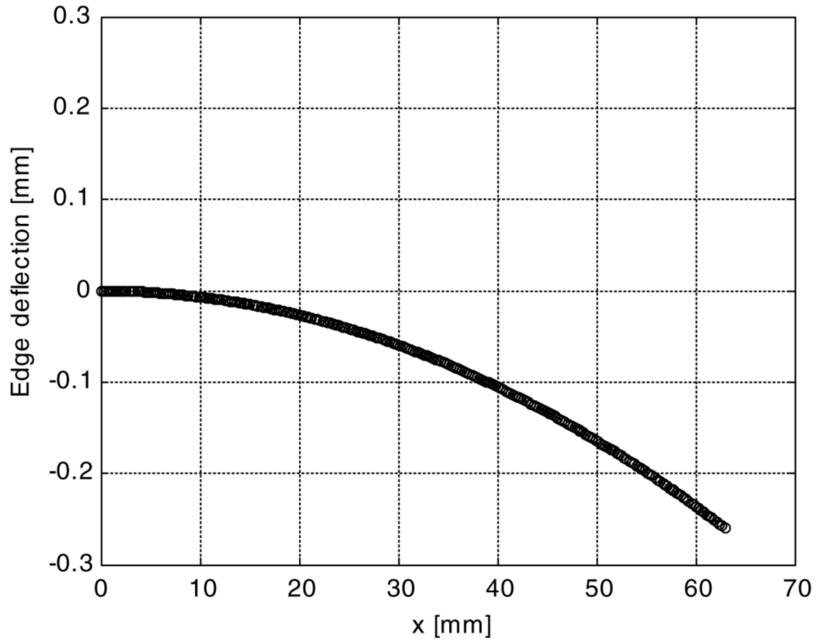

(b)

Edge Deflections (90-direction)

Uniform ΔT of 100°C

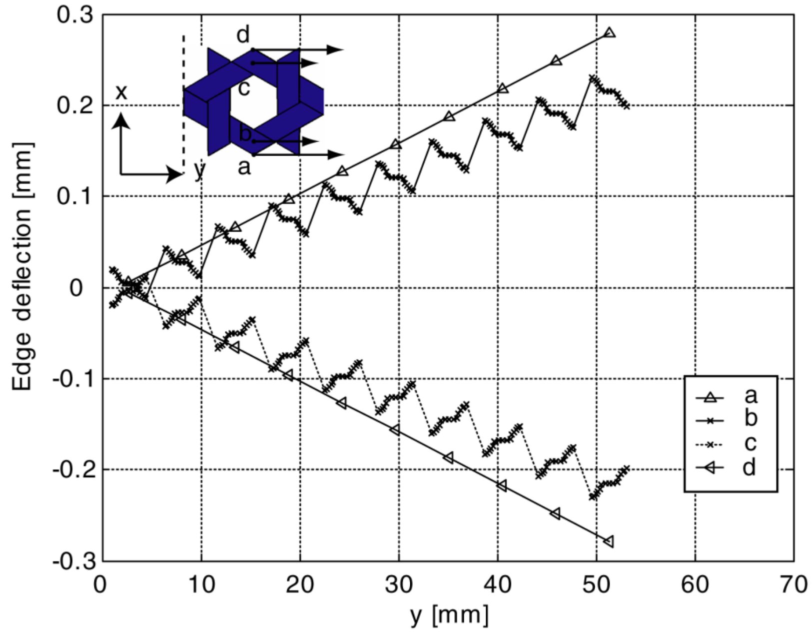

Gradient of +/- 2°C

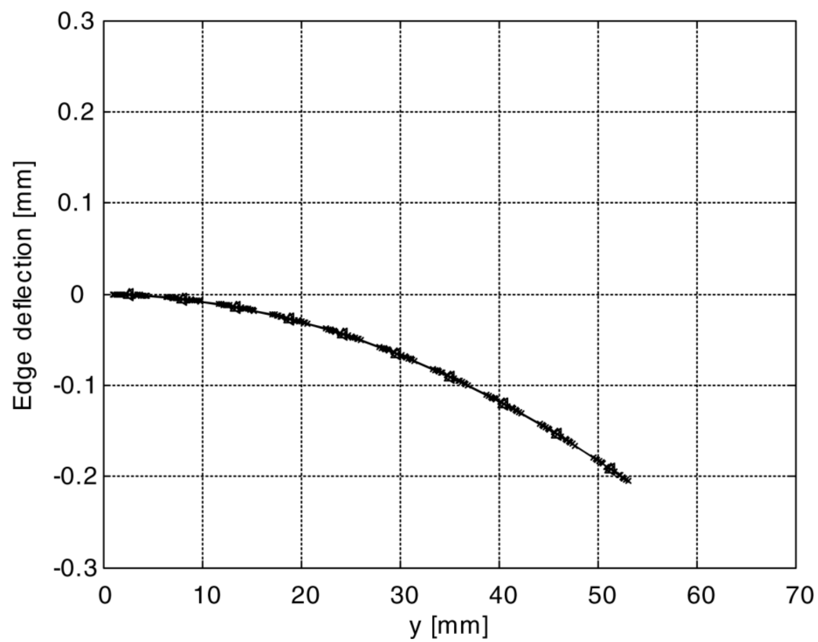

CTT Comparison

- Predicted values for 0- and 90-direction strips are
  -7.168×10^{-5}/ mm ^{o}C and
  -8.128×10^{-5} /mm ^{o}C
- Measured values are
  -7.082×10^{-5}/ mm ^{o}C and
  -9.010×10^{-5} /mm ^{o}C